JOURNAL OF MATERIALS SCIENCE **40** (2005) 2795–2802

On the design of controlled tricrystal specimens for the systematic investigation of static grain boundary triple junction properties

R. KREMER, R. NARAYANAN, S. SHEKHAR, A. H. KING*
School of Materials Engineering, Purdue University, West Lafayette, IN 47907-2044, USA
E-mail: alexking@ecn.purdue.edu

We consider the optimal design of tricrystal specimens for use in experimental studies of static triple junction properties. Important considerations in this regard are the stability and reproducibility of the tricrystal structure, and we develop a straightforward criterion for the selection of particular grain boundary misorientations and interfacial planes that meet these needs. A small set of particular cases is proposed to provide representative, reproducible and therefore comparable bases for the experimental study of triple junction properties.

1. Introduction

Triple junctions are the lines at which three interfaces meet, and while they may be quite generic junctions between different types of interface, our focus here is upon the subset of triple junctions that comprise three individual grain boundaries. We designate these as "grain boundary triple junctions" or GBTJs. Grain boundaries, of course, have been a topic of active research for more than half-a-century, but their triple junctions have only recently been investigated in any detail. A summary of known grain boundary triple junction properties and behaviors can be found in the papers contained in a special issue (number 3/4) of Interface Science, Volume 7 [1].

Although interest in GBTJs is growing rapidly, the majority of published findings about their properties is still theoretical or simulational in nature. Relatively few systematic experimental studies have yet been undertaken, and to the best of our knowledge they are restricted to studies of mobility effects, in which controlled tricrystals have been used [2]. There has also been one reported study of diffusion in an uncontrolled triple junction [3], and some isolated observations of GBTJ effects such as segregation [4]. The lack of systematic studies of triple junction properties may be attributed to the complexity of performing experiments on isolated nano-scale defects, and also to the daunting prospect of investigating a defect that may have as many as 23 structural degrees of freedom [5]. The observed variability of GBTJ responses [4] also leads one to suspect that their properties may strongly dependent upon the structural degrees of freedom.

One result of the dearth of experimental information is that there is not yet any resolution to such a basic question as the sign (let alone the magnitude) of the energy associated with a triple junction, which is left in question by the existing computer simulation studies that provide conflicting results [6–8].

Our purpose in this paper, is to define a small set of triple junctions that can be fully characterized using a wide range of techniques, and used for a wide range of different studies such that the results are all comparable to each other. This goal sets a number of critical requirements:

(i) It should be possible for experimental specimens containing the designed junctions to be created reproducibly, with relative ease;
(ii) The junctions should be stable enough to allow for a variety of experiments to be undertaken on them;
(iii) The crystallography of the junctions should make them amenable to study *via* computer simulation, so that theory and experiment can be compared; and
(iv) The designs should provide a wide enough range of parameters to test the effects of varying at least some of the GBTJ degrees of freedom.

Requirement (i) has previously been met for the case of research on grain boundaries, by growing long bicrystal specimens from oriented seeds [9, 10]. These specimens are then sliced to provide large numbers of specimens with nominally identical boundary parameters that have been used to investigate the properties of the grain boundaries in a variety of systematic experiments. A similar approach, using seeded growth of metallic tricrystals in a vertical Bridgman furnace is a viable means of creating a reference set of experimental triple junctions for systematic study.

*Author to whom all correspondence should be addressed.

The satisfaction of requirement (ii) is more complicated, and is the main subject of this paper. The chosen solution to this problem naturally satisfies requirement (iii), and requirement (iv) calls for a number of varied applications of the reasoning set out in the next section.

2. Design considerations for stable GBTJs

2.1. Stability against boundary plane re-orientation

With the use of Bridgman techniques for tricrystal growth, we have good control over the orientations of the three crystals making up the specimen, and also of the growth direction, which is expected to include the direction of the junction itself. We can exert a modest influence over the boundary planes through the design of the tricrystal mold, but we anticipate that local equilibrium considerations at the GBTJ will overwhelm any attempt that we may make to overcome them to enforce any particular set of grain boundary planes. We must therefore work toward GBTJ parameters that result in tricrystals which are intrinsically stable.

The most elementary approximation that can be applied to this problem is that of isotropic and uniform grain boundary energy. Here, the term "isotropic" means that the boundary energy is invariant with changes of boundary plane, at fixed misorientation, and "uniform" means that all grain boundaries have the same energy irrespective of misorientation. The result of these two assumptions is the familiar conclusion that the grain boundaries always meet at the dihedral angle of 120°, and we can freely choose grain boundary planes that meet this requirement.

Herring [11] has given the condition of stability for three interfaces in the form:

$$\sum_{i=1}^{3}\left(\gamma_i t_i + \frac{\partial \gamma_i}{\partial t_i}\right) = 0 \qquad (1)$$

where γ_1, γ_2 and γ_3, are the three surface tensions, t_i is a unit vector in the plane of the ith interface, normal to the line of intersection and pointing away from the line. Despite the accumulation of considerable amounts of grain boundary data, however, we do not have sufficient information about all of the terms of Equation 1 to provide solutions for completely stable triple lines, in general cases. In order to create stable, artificial tricrystals, therefore, we resort to a strategy of satisfying Equation 1 by making it as close as possible to zero, term by term. Thus we require that our triple junctions meet the following requirements:

$$\sum_{i=1}^{3}(\gamma_i t_i) \approx 0 \qquad (2)$$

and

$$\frac{\partial \gamma_1}{\partial t_1} \approx \frac{\partial \gamma_2}{\partial t_2} \approx \frac{\partial \gamma_3}{\partial t_3} \approx 0 \qquad (3)$$

which together satisfy Equation 1. Requirement (2) is equivalent to the usual isotropic approximation, that is often expressed as

$$\frac{\gamma_1}{\sin \Phi_1} = \frac{\gamma_2}{\sin \Phi_2} = \frac{\gamma_3}{\sin \Phi_3} \qquad (4)$$

where the Φ_i are the dihedral angles formed by the grain boundaries. Sufficient information is available about the variation of grain boundary energy with the boundary parameters (see e.g. [12]) to use requirement (2), or Equation 4 to design the appropriate dihedral angles (and hence boundary planes) for a tricrystal embodying a particular set of misorientations. The variation of dihedral angle predicted by this expression has been used to measure the variation of grain boundary energy with boundary parameters, very successfully [13, 14], but it is not clear that this is sufficient to predict an intrinsically stable triple junction.

There is some evidence of a strong preference for symmetrical tilt grain boundary planes in gold thin films, where triple junctions are predominantly aligned parallel to ⟨111⟩ directions common to all three grains [15], and this indicates that the isotropic approximation may not be a sufficient guide in cases of this type. Since we will describe the design of GBTJs with common low-index directions parallel to the junction line, it appears that anisotropy needs to be considered in the design of the triple junctions. so we also impose requirement (3), which is most simply satisfied by ensuring that the individual grain boundary planes are symmetrically disposed with respect to the crystal lattices that they divide. According to Neumann's principle [16], this must define an energy extremum and it is likely to be a minimum.

A complete analysis of the equilibrium of triple junctions, without the simplifying approximations, can be achieved using the capillarity-vector approach developed by Hoffman and Cahn [17, 18]; however, to apply this method in a design scheme it would be necessary to have a complete Wulff-plot for every grain boundary under consideration, and this information is not usually available. Nevertheless, we can draw some fairly general guidelines from the analysis. In particular, it is found that when one or two of the boundaries that comprise a GBTJ are trapped in a low-energy orientation, then the remaining boundary or boundaries can freely adopt a range of orientations [5]. This corresponds to a set of cases in which the boundary tensions may be imbalanced, generating a resultant force on the GB, that is balanced by the grain boundary torques through their resistance to the rotation of the trapped boundary planes.

Our strategy is to find tricrystal geometries by searching for dihedral angles that are determined by symmetry considerations rather than by energy considerations. From this set of geometries, we select those tricrystals for which the interfacial energy produces small resultant forces, as determined by Equation 2, since that will produce the least likelihood of rotation away from the symmetric boundary plane. A geometric and energetic analysis of triple junctions that comprise only symmetric tilt boundary planes has been provided by Singh and King [19, 20], and in this paper we use a similar analysis applied to a restricted set of GBTJs.

2.2. Stability against grain boundary dissociation

A significant problem in the creation of GBTJs is that they can decompose spontaneously by forming a new grain, which is usually a twin of one of the three grains that meet at the junction [21–28]. This process is evidently driven by the removal of high-energy interfaces through the creation of lower-energy ones. It is dauntingly difficult to attempt to consider all of the possible dissociations that might occur at a selected GBTJ so, again, we resort to a simplifying assumption. Since dissociation reactions result in the formation of at least one twin boundary in almost all observed cases, we select GBTJs that comprise only coincident-site lattice (CSL) related grain boundaries in which there is no direct path to the formation of a $\Sigma 3$ boundary, *via* a reaction of the type

$$\Sigma A \Rightarrow \Sigma B + \Sigma 3 \tag{5}$$

where A and B are odd integers. This reaction is allowed, geometrically, if

$$\alpha A = 3B \tag{6}$$

where α is also an odd integer whose definition and meaning have been discussed by Gertsman [29]: its value is most frequently unity. In order to avoid complications from this type of reaction, we seek wherever possible to select cases in which the Σ-values of any product boundaries are larger than those of the intended tricrystal design. This design criterion requires us to use CSL-related grain boundaries with relatively low Σ-values, meaning that the boundaries have short-range periodic structures. This requirement has the specific benefit of helping to make the structures amenable to study by computer simulation: it does not necessarily predict any specific energetic outcome, though we note that all of the reported experimental observations of this type of reaction result in the production of boundary segments with lower Σ-values than those of the parent segments.

2.3. Selection of a suitable range of GBTJ parameters

In order to provide a reasonable variety of GBTJ parameters, without becoming overwhelmed by the wide range of possibilities, we have narrowed our consideration to three distinct cases: each of them is defined by a common low-index direction of all three grains, lying parallel to the intended GBTJ line direction. As described below, we have designed experimental GBTJ specimens with common ⟨100⟩, ⟨110⟩ and ⟨111⟩ directions. At this relatively early stage of experimental research of GBTJs this narrow range of choices is sufficient to provide some baseline information, although it is not likely to be readily extendable to more general cases. If the rules provided here are successful, then our approach can subsequently be extended to more general cases.

3. GBTJ design specifics

For each triple junction axis, we identify all of the available CSLs, and triple junctions that can be constructed from them, typically using Σ-values up to 99. Each CSL provides up to two distinct possible symmetric tilt grain boundary planes, as described below, and these planes provide sets of possible dihedral angles, which are evaluated by determining the resultant force applied to the GBTJs by the three directed grain boundary tensions. Those GBTJs whose symmetrical boundary planes produce the smallest resultant force are selected as the ones most likely to be stable. In order to simplify this process, triple junctions that include dihedral angles greater than 180° are excluded *a priori*, since they must produce a large resultant force. We note that despite this large force, GBTJs of this type have been observed and analyzed in detail [30], demonstrating that the torque terms in Equation 1 may be significant.

We have used grain boundary energies taken from simulation studies by Wolf, using Lennard-Jones (LJ) and embedded atom method (EAM) interatomic potentials [31].

3.1. ⟨100⟩ junctions

Details of all of the GBTJs that were evaluated are shown in Table I. For each of the CSLs produced by rotations about ⟨100⟩ in cubic materials, there are four specific symmetric tilt grain boundary planes, and these correspond to the edges and the diagonals of the CSL unit cell, when viewed in the [100] projection, as shown in Fig. 1. The boundaries produced by the two CSL edges are equivalent to each other, and produce physically identical GBTJs, and the two diagonal boundary planes produce a similar degeneracy, so we consider only one of the two cases in each class. It is possible, however to mix the "edge" and "diagonal" boundary planes from the different CSLs in making up the triple junction. In each case, for three specific misorientations, there are two distinct sets of symmetrical tilt boundary planes, giving rise to two distinct triple junctions, which have the same (symmetry-determined) dihedral angles. The two cases are related by a 45° rotation of all three of the boundary planes about the axis of the GBTJ. Resultant forces for both configurations are shown in the table.

The resultant forces predicted for the [100] symmetrical triple junctions range from 0.058 to 0.139 N/m based on Wolf's LJ results, and from 0.022 to 0.158 N/m using the EAM data.

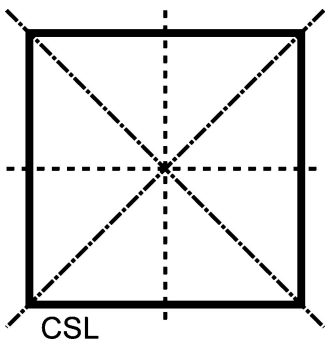

Figure 1 The orientations of symmetric tilt grain boundary planes relative to the CSL unit cell, for [100] grain boundaries of interest in this work. Similar styles of broken line indicate boundaries that are symmetrically equivalent to each other.

TABLE I Candidate triple junctions with a common [100] axis. The lowest resultant force values are indicated in bold type, and the junction selected as the best candidate for further study is indicated by underlined resultant force values. In this case, the LJ and the EAM computations predict different choices, but the GBTJ chosen on the basis of the EAM calculation is the second-ranked choice for the LJ computation, and this appears, overall, to be a sound choice

	GB 1	GB 2	GB 3	Resultant force on TJ, (N/m)
CSL, θ	$\Sigma 5$, 36.87°	$\Sigma 5$, 36.87°	$\Sigma 25$, 16.26°	
GB Plane	{031}	{031}	{017}	
GB Energy (J/m^2)	0.87_{lj}; 0.84_{eam}	0.87_{lj}; 0.84_{eam}	0.83_{lj}; 0.73_{eam}	$\underline{0.058}_{lj}$; $\underline{\mathbf{0.022}}_{eam}$
Alternate GB plane	{021}	{021}	{034}	
Alt GB Energy (J/m^2)	0.92_{lj}; 0.88_{eam}	0.92_{lj}; 0.88_{eam}	0.73_{lj}; 0.63_{eam}	0.090_{lj}; 0.158_{eam}
Dihedral Angle	116.57°	116.57°	126.87°	
CSL, θ	$\Sigma 5$, 36.87°	$\Sigma 13$, 22.62°	$\Sigma 65$a, 30.51°	
GB Plane	{013}	{015}	{0 3 11}	
GB Energy (J/m^2)	0.87_{lj}; 0.84_{eam}	0.90_{lj}; 0.81_{eam}	0.92_{lj}; 0.86_{eam}	0.090_{lj}; 0.045_{eam}
Alternate GB plane	{021}	{032}	{047}	
Alt GB Energy (J/m^2)	0.92_{lj}; 0.88_{eam}	0.82_{lj}; 0.72_{eam}	0.90_{lj}; 0.83_{eam}	$\mathbf{0.035}_{lj}$; 0.091_{eam}
Dihedral Angle	116.57°	123.69°	119.74°	
CSL, θ	$\Sigma 5$, 53.13°	$\Sigma 13$, 22.62°	$\Sigma 65$b, 14.25°	
GB Plane	{021}	{015}	{081}	
GB Energy (J/m^2)	0.92_{lj}; 0.88_{eam}	0.90_{lj}; 0.81_{eam}	0.81_{lj}; 0.70_{eam}	0.139_{lj}; 0.058_{eam}
Alternate GB plane	{031}	{023}	{079}	
Alt GB Energy (J/m^2)	0.87_{lj}; 0.84_{eam}	0.82_{lj}; 0.72_{eam}	0.68_{lj}; 0.59_{eam}	0.096_{lj}; 0.109_{eam}
Dihedral Angle	108.52°	123.96°	127.52°	
CSL, θ	$\Sigma 25$, 16.26°	$\Sigma 65$a, 59.48°	$\Sigma 65$b, 14.25°	
GB Plane	{017}	{047}	{081}	
GB Energy (J/m^2)	0.83_{lj}; 0.73_{eam}	0.90_{lj}; 0.83_{eam}	0.81_{lj}; 0.70_{eam}	0.085_{lj}; 0.041_{eam}
Alternate GB plane	{034}	{0 3 11}	{079}	
Alt GB Energy (J/m^2)	0.73_{lj}; 0.63_{eam}	0.92_{lj}; 0.86_{eam}	0.68_{lj}; 0.59_{eam}	0.061_{lj}; 0.129_{eam}
Dihedral Angle	122.22°	106.47°	131.41°	

In this case, the LJ and the EAM computations predict different choices, but the GBTJ chosen on the basis of the EAM calculation is the second-ranked choice for the LJ computation, and this appears, overall, to be a sound choice. The junction selected as the most suitable for experimental study, is indicated by underlining in the table, and is illustrated in Fig. 2.

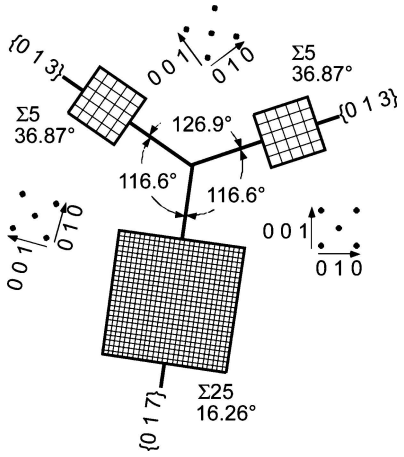

Figure 2 Geometrical details for the [100] triple junction selected as the most likely to be stable.

3.2. ⟨110⟩ junctions

Details of all of the GBTJs that were evaluated for the ⟨110⟩ axis are shown in Table II. For this axis, the CSLs have orthorhombic unit cells, and there are only two symmetric tilt boundaries which contain the primary rotation axis. These correspond to the long and short edges of the CSL, when viewed in a ⟨110⟩ projection, as shown in Fig. 3. The two boundary planes are distinct symmetrical configurations oriented at 90° to each other. Thus for each GBTJ configuration, comprising three fixed misorientations, there are two symmetry-related symmetric tilt configurations, which are related by a 90° rotation of all three boundary planes about the common rotation axis.

The resultant forces predicted for these symmetrical triple junctions range from 0.007 to 0.457 N/m based on Wolf's LJ results, and from 0.056 to 0.441 N/m using the EAM data.

The junction selected as the most suitable for experimental study, is indicated by underlining in the table, and is illustrated in Fig. 4.

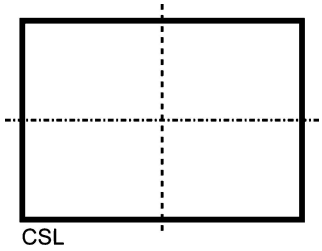

Figure 3 The orientations of symmetric tilt grain boundary planes relative to the CSL unit cell, for [110] grain boundaries of interest in this work.

TABLE II Candidate triple junctions with a common [110] axis. The lowest resultant force values are indicated in bold type, and the junction selected as the best candidate for further study is indicated by underlined resultant force values. In this case the LJ and EAM results suggest the same triple junction as the most suitable for further study

	GB 1	GB 2	GB 3	Resultant force on TJ (N/m)
CSL, θ	$\Sigma 9$: 141.06°	$\Sigma 9$: 141.06°	$\Sigma 81$: 77.88°	
GB Plane	{1 1 4}	{1 1 4}	{7 7 8}	
GB Energy (J/m^2)	0.70_{lj}; 0.56_{eam}	0.70_{lj}; 0.56_{eam}	0.47_{lj}; 0.43_{eam}	$\underline{\mathbf{0.007}}_{lj}$; $\underline{\mathbf{0.056}}_{eam}$
Alternate GB plane	{2 2 1}	{2 2 1}	{4 4 7}	
Alt GB Energy (J/m^2)	0.75_{lj}; 0.77_{eam}	0.75_{lj}; 0.77_{eam}	0.60_{lj}; 0.59_{eam}	0.100_{lj}; 0.077_{eam}
Dihederal angle	109.47°	109.47°	141.06°	
CSL, θ	$\Sigma 9$: 141.06°	$\Sigma 11$: 129.52°	$\Sigma 99a$: 89.42°	
GB Plane	{1 1 4}	{1 1 3}	{5 5 7}	
GB Energy (J/m^2)	0.70_{lj}; 0.56_{eam}	0.36_{lj}; 0.29_{eam}	0.66_{lj}; 0.54_{eam}	0.383_{lj}; 0.307_{eam}
Alternate GB plane	{2 2 1}	{3 3 2}	{7 7 10}	
Alt GB Energy (J/m^2)	0.75_{lj}; 0.77_{eam}	0.70_{lj}; 0.65_{eam}	0.66_{lj}; 0.54_{eam}	0.111_{lj}; 0.084_{eam}
Dihederal angle	109.47°	115.24°	135.29°	
CSL, θ	$\Sigma 9$: 141.06°	$\Sigma 11$: 50.48°	$\Sigma 99b$: 168.46°	
GB Plane	{1 1 4}	{3 3 2}	{1 1 14}	
GB Energy (J/m^2)	0.70_{lj}; 0.56_{eam}	0.70_{lj}; 0.65_{eam}	0.59_{lj}; 0.49_{eam}	0.457_{lj}; 0.441_{eam}
Alternate GB plane	{2 2 1}	{1 1 3}	{7 7 1}	
Alt GB Energy (J/m^2)	0.75_{lj}; 0.77_{eam}	0.36_{lj}; 0.29_{eam}	0.66_{lj}; 0.61_{eam}	0.143_{lj}; 0.191_{eam}
Dihederal angle	109.47°	154.76°	95.77°	
CSL, θ	$\Sigma 9$: 141.06°	$\Sigma 33a$: 58.99°	$\Sigma 33c$: 159.95°	
GB Plane	{1 1 4}	{5 5 4}	{1 1 8}	
GB Energy (J/m^2)	0.70_{lj}; 0.56_{eam}	0.51_{lj}; 0.46_{eam}	0.78_{lj}; 0.62_{eam}	0.153_{lj}; 0.159_{eam}
Alternate GB plane	{2 2 1}	{2 2 5}	{4 4 1}	
Alt GB Energy (J/m^2)	0.75_{lj}; 0.77_{eam}	0.58_{lj}; 0.48_{eam}	0.80_{lj}; 0.75_{eam}	0.248_{lj}; 0.109_{eam}
Dihederal angle	109.47°	150.5°	100.03°	

3.3. ⟨111⟩ junctions

Details of all of the GBTJs that were evaluated for the ⟨111⟩ axis are shown in Table III. For this axis, the CSLs have hexagonal unit cells, with 3-fold symmetry, and there are three symmetric tilt boundaries for each misorientation about the primary rotation axis. These boundary planes are either parallel (for $\Sigma = 3N$) or perpendicular (for $\Sigma \neq 3N$) to the prism faces of the CSL unit cells, as shown in Fig. 5, and are structurally equivalent to each other. For this axis, therefore, there is only a single symmetric GBTJ configuration for each set of misorientations.

Other boundary planes are related to symmetric tilt boundaries, through the addition of a "double-positioning" inversion, as described by Singh and King [15]. These boundary planes occur at orientations 30° away from the true symmetric boundary orientations, but still contain the GBTJ axis in their planes. Although these boundaries have been shown experimentally to have low energy, they have not been the subject of any simulation studies of which we are aware, so we are unable to include them in the present analysis. For each true symmetric GBTJ structure, there is double-positioned symmetric GBTJ structure, with identical dihedral angles, created by rotating all three boundary planes by 30° about the GBTJ line, and there are also many possible structures that involve mixtures of true- and double-positioned symmetric tilt grain boundaries, such as those observed by Singh and King, but these are not evaluated here.

The resultant forces predicted for the true symmetrical triple junctions range from 0.157 to 0.503 N/m based on Wolf's LJ results, and from 0.113 to 0.451 N/m using the EAM data.

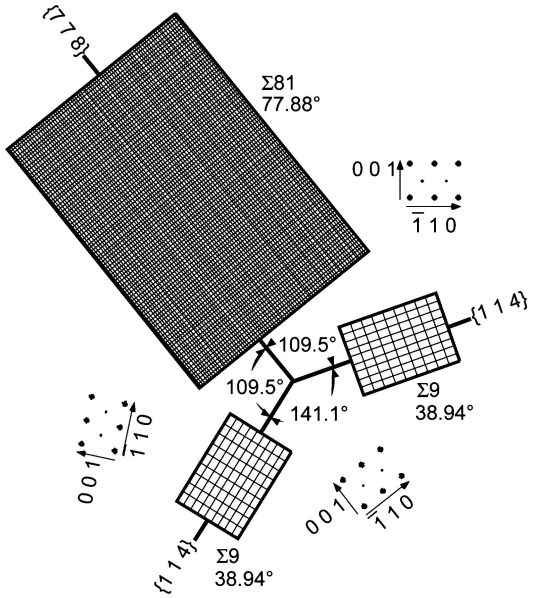

Figure 4 Geometrical details for the [110] triple junction selected as the most likely to be stable.

In this case, the LJ and the EAM computations predict different choices. The two junctions selected as likely to be stable are shown in boldface in the table, and illustrated in Figs 6 and 7. The GBTJ selected on the basis of the LJ calculations (illustrated in Fig. 6) includes a $\Sigma 3$ twin boundary and is likely to be a special case in some respects.

TABLE III Candidate triple junctions with a common [111] axis. The lowest resultant force values are indicated in bold type, and the junction selected as the best candidate for further study is indicated by underlined resultant force values. In this case, the LJ and the EAM computations predict different choices. We make our selection on the basis that the EAM calculation is likely to be more accurate, and also that the chosen junction does not include a Σ3 interface, which is likely to exhibit somewhat special behavior

	GB 1	GB 2	GB 3	Resultant force on TJ (N/m)
CSL, θ	Σ3, 60.00°	Σ7, 32.21°	Σ21, 21.79°	
GB Plane	{1 1 2}	{1 2 3}	{1 4 5}	
GB Energy (J/m^2)	0.60_{lj}; 0.50_{eam}	0.89_{lj}; 0.81_{eam}	0.82_{lj}; 0.72_{eam}	0.214_{lj}; 0.138_{eam}
Dihederal angle	150.0°	79.1°	130.9°	
CSL, θ	Σ3, 60.00°	Σ7, 32.21°	Σ21, 21.79°	
GB Plane	{1 1 2}	{1 2 3}	{1 4 5}	
GB Energy (J/m^2)	0.60_{lj}; 0.50_{eam}	0.89_{lj}; 0.81_{eam}	0.82_{lj}; 0.72_{eam}	$\mathbf{0.157}_{lj}$; 0.121_{eam}
Dihederal angle	150°	100.9°	109.1°	
CSL, θ	Σ3, 60.00°	Σ7, 32.21°	Σ21, 21.79°	
GB Plane	{1 1 2}	{1 2 3}	{1 4 5}	
GB Energy (J/m^2)	0.60_{lj}; 0.50_{eam}	0.89_{lj}; 0.81_{eam}	0.82_{lj}; 0.72_{eam}	0.410_{lj}; 0.376_{eam}
Dihederal angle	150°	139.1°	70.9°	
CSL, θ	Σ3, 60.00°	Σ7, 32.21°	Σ21, 21.79°	
GB Plane	{1 1 2}	{1 2 3}	{1 4 5}	
GB Energy (J/m^2)	0.60_{lj}; 0.50_{eam}	0.89_{lj}; 0.81_{eam}	0.82_{lj};0.72_{eam}	0.503_{lj}; 0.400_{eam}
Dihederal angle	150°	40.9°	169.1°	
CSL, θ	Σ7, 38.21°	Σ7, 38.21°	Σ49, 43.57°	
GB Plane	{1 2 3}	{1 2 3}	{3 5 8}	
GB Energy (J/m^2)	0.89_{lj}; 0.81_{eam}	0.89_{lj}; 0.81_{eam}	0.90_{lj}; 0.83_{eam}	0.450_{lj}; 0.404_{eam}
Dihederal angle	139.1°	139.1°	81.8°	
CSL, θ	Σ7, 38.21°	Σ7, 38.21°	Σ49, 43.57°	
GB Plane	{1 2 3}	{1 2 3}	{3 5 8}	
GB Energy (J/m^2)	0.89_{lj}; 0.81_{eam}	0.89_{lj}; 0.81_{eam}	0.90_{lj}; 0.83_{eam}	0.491_{lj}; 0.451_{eam}
Dihederal angle	139.1°	79.1°	141.8°	
CSL, θ	Σ21, 21.79°	Σ21, 21.79°	Σ49, 43.57°	
GB Plane	{1 4 5}	{1 4 5}	{3 5 8}	
GB Energy (J/m^2)	0.82_{lj}; 0.72_{eam}	0.82_{lj}; 0.72_{eam}	0.90_{lj}; 0.83_{eam}	$\underline{0.174}_{lj}$; $\underline{\mathbf{0.113}}_{eam}$
Dihederal angle	130.9°	130.9°	98.2°	
CSL, θ	Σ21, 21.79°	Σ21, 21.79°	Σ49, 43.57°	
GB Plane	{1 4 5}	{1 4 5}	{3 5 8}	
GB Energy (J/m^2)	0.82_{lj}; 0.72_{eam}	0.82_{lj}; 0.72_{eam}	0.90_{lj}; 0.83_{eam}	0.364_{lj}; 0.356_{eam}
Dihederal angle	109.1°	109.1°	141.8°	

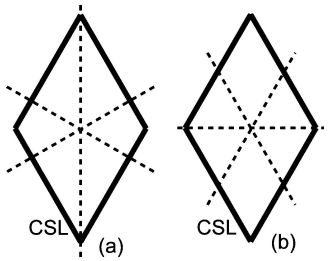

Figure 5 The orientations of symmetric tilt grain boundary planes relative to the CSL unit cell, for [111] grain boundaries of interest in this work. (a) Shows the case for grain boundaries where Σ is not a multiple of 3, and (b) is the case for $\Sigma = 3N$. The figures can be read conversely as showing the orientations of double-positioned symmetric tilt boundaries for $\Sigma = 3N$ in (a) and $\Sigma \neq 3N$ in (b).

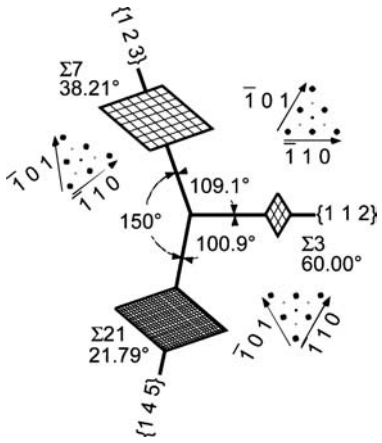

Figure 6 Geometrical details for a [111] triple junction selected as the most likely to be stable.

4. Discussion

The LJ and EAM potentials yield slightly differing results but do not significantly impact the choice of suitable GBTJs for further study. This is because the balance of grain boundary energies is unaffected if all of the boundary energies change by the same factor, going from one method to another. The particular use to which we have put the energies is therefore insensitive to the absolute energy results, but quite sensitive to the relative values among the boundaries.

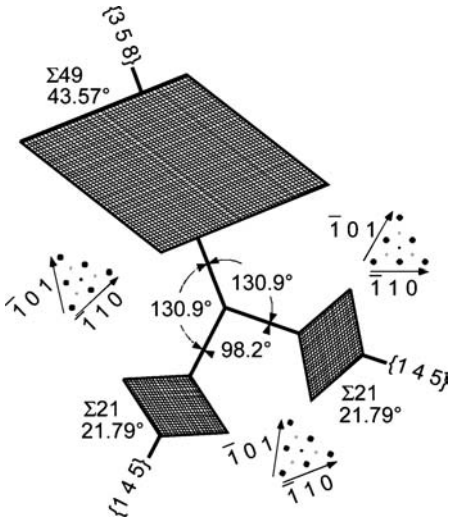

Figure 7 Geometrical details for an alternate [111] triple junction selected to be likely to be stable, and not incorporate a Σ3 boundary.

The fact that the simulations were carried out at a temperature of zero Kelvin is expected to have a similarly small impact on the ranking of the GBTJ stabilities: this would only cause a substantial error if the interfacial entropy displayed large variations from boundary to boundary, causing significant variations in the temperature-dependence of the interfacial free energy. Too little is yet known about interfacial entropy to assess its impact in the present application.

In general, the ⟨100⟩ symmetric tilt triple junctions exhibit small resultant forces relative to those of the ⟨110⟩ and ⟨111⟩ cases, although the smallest resultant force that we have found in this survey is for a ⟨110⟩ junction. The ⟨111⟩ junctions generally exhibit large residual forces, although we note that a strong preference for symmetric tilt triple junctions was first observed for the case of ⟨111⟩ junctions, in gold [15]. We are therefore reasonably confident that most of the junctions that are specified in Tables I–III retain the possibility of being stable with respect to rotations of the boundary planes.

Stability against the formation of twins, however, is a greater problem in the ⟨110⟩ and ⟨111⟩ triple junctions. In many cases, here, at least one of the boundaries is characterized by a Σ-value that is an integer multiple of 3, and therefore twin-forming reactions are geometrically very straightforward. Since the energy of the Σ3 twin is especially low on the coherent {111} plane, reactions that form twins on that plane are of particular concern to us here, and this is especially a problem in the case of the ⟨110⟩ triple junctions, where a low-energy twin boundary can be formed parallel to the intended GBTJ line, as illustrated in Fig. 8.

Despite the uncertainties of our results, there is a very close similarity between the EAM predictions, which are specific to copper, and the LJ predictions, which are more generically appropriate to FCC metals. We therefore believe that the GBTJ designs given here will be appropriate for other FCC metals. It is not clear whether the same geometries would be predicted for any BCC metals.

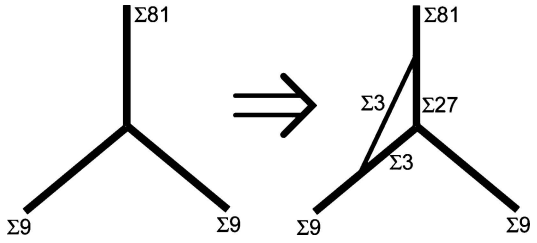

Figure 8 Possible dissociation of a triple junction to form a twin, with its boundary lying parallel to the intended junction. The likelihood of this kind of dissociation is reduced by avoiding boundaries for which $\Sigma = 3N$.

5. Summary

The triple junctions specified in Tables I–III are suitable candidates for detailed experimental and simulational studies, since they are likely to be stable against reorientation or dissociation. The junctions that exhibit the lowest resultant forces will be the most stable.

Other potentially stable triple junctions may be found for the ⟨111⟩ axis, incorporating double-positioned symmetric tilt boundaries, but there is not sufficient information about the energy of this class of interface to enable us to incorporate them into the present design scheme.

A remaining concern, suitable for further experimental study, is the formation of twins, especially in the case of the ⟨110⟩ triple junctions.

Acknowledgment

This work is supported by the US Department of Energy, under contract number DE-FG01-01ER45940.

References

1. G. GOTTSTEIN, A. KING and L. SHVINDLERMAN, *Interf. Sci.* **7** (1999) 215.
2. U. CZUBAYKO, V. G. SURSAEVA, G. GOTTSTEIN and L. S. SHVINDLERMAN, in "Grain Growth in Polycrystalline Materials III", edited by H. Weiland, B. L. Adams and A. D. Rollett (TMS, 1998) p. 423.
3. B. BOKSTEIN, V. IVANOV, O. ORESHINA, A. PETELINE and S. PETELINE, *Mater. Sci. and Engng. a-Struct. Mater. Propert. Microstr. Process.* **302** (2001) 151.
4. K. M. YIN, A. H. KING, T. E. HSIEH, F. R. CHEN, J. J. KAI and L. CHANG, *Micros. Microanal.* **3** (1997) 417.
5. A. H. KING, *Interf. Sci.* **7** (1999) 251.
6. S. G. SRINIVASAN, J. W. CAHN, H. JONSSON and G. KALONJI, *Acta Materialia* **47** (1999) 2821.
7. O. A. SHENDEROVA and D. W. BRENNER, *Phys. Rev.* B **60** (1999) 7053.
8. A. CARO and H. VAN SWYGENHOVEN, *ibid.* **6313**, art. no. (2001).
9. F. S. CHEN and A. H. KING, *Acta Metallurgica* **36** (1988) 2827.
10. S. M. SCHWARZ, E. C. HOUGE, L. A. GIANNUZZI and A. H. KING, *J. Cryst. Growth* **222** (2001) 392.
11. C. HERRING, in "The Physics of Powder Metallurgy", edited by W. E. Kingston (McGraw-Hill, 1949) p. 143.
12. D. WOLF and K. L. MERKLE, in "Mater. Interfaces: Atomic-Level Structure and Properties", edited by D. Wolf and S. Yip (Chapman & Hall, London, 1992) p. 87.
13. N. A. GJOSTEIN and F. N. RHINES, *Acta Metallurgica* **7** (1959) 319.
14. B. L. ADAMS, S. TA'ASAN, D. KINDERLEHRER, I. LIVSHITS, D. E. MASON, C. T. WU, W. W.

MULLINS, G. S. ROHRER, A. D. ROLLETT and D. M. SAYLOR, *Interf. Sci.* **7** (1999) 321.
15. V. SINGH and A. H. KING, *Scripta Materialia* **34** (1996) 1723.
16. F. E. NEUMANN, "Vorlesungen uber die Theorie der Elasticitat" (Teubner, Leipzig, 1885).
17. D. W. HOFFMAN and J. W. CAHN, *Surf. Sci.* **31** (1972) 368.
18. J. W. CAHN and D. W. HOFFMAN, *Acta Metall.* **22** (1974) 1205.
19. V. V. SINGH, Ph.D. Dissertation: Grain Boundary Networks in Thin Metal Films, State University of New York, Stony Brook, 1997.
20. A. H. KING and V. SINGH, in "Intergranular and Interphase Boundaries in Materials., Pt 1" (Transtec Publications Ltd, Zurich-Uetikon, 1996) p. 257.
21. P. J. GOODHEW, T. Y. TAN and R. W. BALLUFFI, *Acta Metall.* **26** (1978) 557.
22. L. M. CLAREBROUGH and C. T. FORWOOD, *Phys. Status Solidi a-Appl. Res.* **104** (1987) 51.
23. *Idem. ibid.* **60** (1980) 51.
24. L. K. FIONOVA, A. V. ANDREEVA and T. I. ZHUKOVA, *ibid.* **67** (1981) K15.
25. C. T. FORWOOD and L. M. CLAREBROUGH, *Acta Metallurgica.* **32** (1984) 757.
26. V. N. PEREVEZENTSEV and M. Y. SHCHERBAN, *Physica. Status Solidi A* **88** (1985) 421.
27. D. L. MEDLIN, S. M. FOILES and D. COHEN, *Acta Materialia* **49** (2001) 3689.
28. U. DAHMEN, C. J. D. HETHERINGTON, V. RADMILOVIC, E. JOHNSON, S. Q. XIAO and C. P. LUO, *Microsc. Microanal.* **8** (2002) 247.
29. V. Y. GERTSMAN, *Acta Crystallogr. Sec.* A **57** (2001) 369.
30. A. H. KING, F. R. CHEN, L. CHANG and J. J. KAI, *Interf. Sci.* **5** (1997) 287.
31. D. WOLF, *Acta Metallurgica et Materialia* **38** (1990) 781.